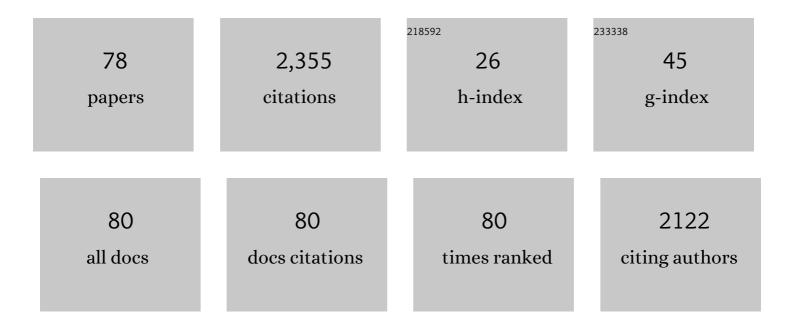
List of Publications by Year in descending order

Source: https://exaly.com/author-pdf/821198/publications.pdf Version: 2024-02-01



#	Article	IF	CITATIONS
1	Predicting the formation and stability of single phase high-entropy alloys. Acta Materialia, 2016, 104, 172-179.	3.8	283
2	High-Entropy Alloys for Advanced Nuclear Applications. Entropy, 2021, 23, 98.	1.1	131
3	Segregation and migration of species in the CrCoFeNi high entropy alloy. Journal of Alloys and Compounds, 2014, 599, 179-182.	2.8	126
4	Synthesis and DFT investigation of new bismuth-containing MAX phases. Scientific Reports, 2016, 6, 18829.	1.6	97
5	Swelling due to fission products and additives dissolved within the uranium dioxide lattice. Journal of Nuclear Materials, 2012, 427, 359-363.	1.3	90
6	Accommodation, Accumulation, and Migration of Defects in <scp><scp>Ti</scp></scp> ₃ <scp>SiC</scp> ₂ and <scp><scp>Ti</scp></scp> 3 <scp>AIC</scp> ₂ MAX Phases. Journal of the American Ceramic Society, 2013, 96, 3196-3201.	1.9	73
7	Phase equilibria in the U-Si system from first-principles calculations. Journal of Nuclear Materials, 2016, 479, 216-223.	1.3	68
8	Accommodation of Excess Oxygen in Group II Monoxides. Journal of the American Ceramic Society, 2013, 96, 308-311.	1.9	67
9	Modelling the thermal conductivity of (U Th1â^')O2 and (U Pu1â^')O2. Journal of Nuclear Materials, 2015, 466, 29-35.	1.3	65
10	Non-stoichiometry in U3Si2. Journal of Nuclear Materials, 2016, 482, 300-305.	1.3	64
11	High temperature, low neutron cross-section high-entropy alloys in the Nb-Ti-V-Zr system. Acta Materialia, 2019, 166, 435-446.	3.8	60
12	Gradual Structural Evolution from Pyrochlore to Defect-Fluorite in Y ₂ Sn _{2–<i>x</i>} Zr _{<i>x</i>} O ₇ : Average vs Local Structure. Journal of Physical Chemistry C, 2013, 117, 26740-26749.	1.5	54
13	Hydrogen induced vacancy formation in tungsten. Journal of Nuclear Materials, 2014, 448, 270-275.	1.3	47
14	Defects and transport processes in beryllium. Acta Materialia, 2011, 59, 7095-7103.	3.8	44
15	Solution of trivalent cations into uranium dioxide. Journal of Nuclear Materials, 2012, 420, 258-261.	1.3	44
16	The incorporation of plutonium in lanthanum zirconate pyrochlore. Journal of Nuclear Materials, 2013, 443, 444-451.	1.3	44
17	Density functional theory calculations of self- and Xe diffusion in U3Si2. Journal of Nuclear Materials, 2019, 515, 312-325.	1.3	43
18	Atomic Scale Modeling of Point Defects in Zirconium Diboride. Journal of the American Ceramic Society, 2011, 94, 2225-2229.	1.9	34

#	Article	IF	CITATIONS
19	Predicting the Crystal Structure and Phase Transitions in High-Entropy Alloys. Jom, 2015, 67, 2375-2380.	0.9	33
20	Raman spectroscopic study of natural and synthetic brannerite. Journal of Nuclear Materials, 2013, 437, 149-153.	1.3	31
21	The formation and structure of Fe-Mn-Ni-Si solute clusters and G-phase precipitates in steels. Journal of Nuclear Materials, 2018, 505, 1-6.	1.3	31
22	Solution of hydrogen in accident tolerant fuel candidate material: U3Si2. Journal of Nuclear Materials, 2018, 501, 234-237.	1.3	31
23	Novel Chemical Synthesis and Characterization of CeTi2O6 Brannerite. Inorganic Chemistry, 2014, 53, 6761-6768.	1.9	30
24	Crystallographic evolution of MAX phases in proton irradiating environments. Journal of Nuclear Materials, 2018, 502, 220-227.	1.3	30
25	The stability of irradiation-induced defects in Zr3AlC2, Nb4AlC3 and (Zr0.5,Ti0.5)3AlC2 MAX phase-based ceramics. Acta Materialia, 2020, 183, 24-35.	3.8	29
26	Thermal conductivity and energetic recoils in UO ₂ using a many-body potential model. Journal of Physics Condensed Matter, 2014, 26, 495401.	0.7	28
27	Interface properties of Ti3SiC2/Al2O3 ceramics: Combined experiments and first-principles calculations. Ceramics International, 2021, 47, 6409-6417.	2.3	28
28	Accommodation of excess oxygen in fluorite dioxides. Solid State Ionics, 2013, 253, 119-122.	1.3	27
29	Uranium nitride-silicide advanced nuclear fuel: higher efficiency and greater safety. Advances in Applied Ceramics, 2018, 117, s76-s81.	0.6	26
30	Peroxide defect formation in zirconate perovskites. Journal of Materials Chemistry A, 2014, 2, 15883-15888.	5.2	25
31	Stoichiometry deviation in amorphous zirconium dioxide. RSC Advances, 2019, 9, 16320-16327.	1.7	25
32	Spark plasma sintering and microstructural analysis of pure and Mo doped U 3 Si 2 pellets. Journal of Nuclear Materials, 2017, 496, 234-241.	1.3	23
33	Structural stability and fission product behaviour in U3Si. Journal of Nuclear Materials, 2015, 466, 739-744.	1.3	22
34	Formation and structure of V–Zr amorphous alloy thin films. Acta Materialia, 2015, 83, 269-275.	3.8	21
35	Partition of soluble fission products between the grey phase, ZrO2 and uranium dioxide. Journal of Nuclear Materials, 2013, 438, 238-245.	1.3	19
36	Theoretical and experimental Raman spectroscopic studies of synthetic thorutite (ThTi2O6). Journal of Nuclear Materials, 2014, 446, 68-72.	1.3	19

#	Article	IF	CITATIONS
37	Anisotropy in the thermal expansion of uranium silicide measured by neutron diffraction. Journal of Nuclear Materials, 2018, 508, 516-520.	1.3	19
38	DFT study of the hexagonal high-entropy alloy fission product system. Journal of Nuclear Materials, 2017, 488, 70-74.	1.3	18
39	Defect evolution in burnable absorber candidate material: Uranium diboride, UB2. Journal of Nuclear Materials, 2019, 513, 45-55.	1.3	18
40	Structure, properties and formation of PuCrO3 and PuAlO3 of relevance to doped nuclear fuels. Journal of Materials Chemistry A, 2013, 1, 14633.	5.2	17
41	Formation of (Cr,Al)UO4 from doped UO2 and its influence on partition of soluble fission products. Journal of Nuclear Materials, 2013, 443, 236-241.	1.3	16
42	Technetium and ruthenium incorporation into rutile TiO2. Journal of Nuclear Materials, 2013, 441, 380-389.	1.3	16
43	Atomic scale modelling of hexagonal structured metallic fission product alloys. Royal Society Open Science, 2015, 2, 140292.	1.1	16
44	Choosing the correct strong correlation correction for U3Si2: Influence of magnetism. Journal of Nuclear Materials, 2019, 527, 151828.	1.3	16
45	UN microspheres embedded in UO2 matrix: An innovative accident tolerant fuel. Journal of Nuclear Materials, 2020, 540, 152355.	1.3	16
46	Structure and properties of amorphous uranium dioxide. Acta Materialia, 2021, 202, 366-375.	3.8	16
47	Oxidation of UN/U2N3-UO2 composites: an evaluation of UO2 as an oxidation barrier for the nitride phases. Journal of Nuclear Materials, 2021, 544, 152700.	1.3	16
48	In-situ TEM investigation of nano-scale helium bubble evolution in tantalum-doped tungsten at 800°C. Journal of Nuclear Materials, 2021, 550, 152910.	1.3	16
49	Hydrogen accommodation in -iron and nickel. Journal of Alloys and Compounds, 2014, 587, 794-799.	2.8	15
50	Preferential formation of Al self-interstitial defects in Î ³ -TiAl under irradiation. Intermetallics, 2013, 32, 230-232.	1.8	14
51	Ultrafast palladium diffusion in germanium. Journal of Materials Chemistry A, 2015, 3, 3832-3838.	5.2	14
52	Density functional theory study of the magnetic moment of solute Mn in bcc Fe. Physical Review B, 2018, 98, .	1.1	14
53	Void evolution in tungsten and tungsten-5wt.% tantalum under in-situ proton irradiation at 800 and 1000â€ ⁻ °C. Journal of Nuclear Materials, 2019, 526, 151730.	1.3	13
54	Vacancy mediated cation migration in uranium dioxide: The influence of cluster configuration. Solid State Ionics. 2014, 266, 68-72.	1.3	12

#	Article	IF	CITATIONS
55	Influence of boron isotope ratio on the thermal conductivity of uranium diboride (UB2) and zirconium diboride (ZrB2). Journal of Nuclear Materials, 2020, 528, 151892.	1.3	12
56	Synthesis of candidate advanced technology fuel: Uranium diboride (UB2) via carbo/borothermic reduction of UO2. Journal of Nuclear Materials, 2020, 540, 152388.	1.3	12
57	Crystal structure, thermodynamics, magnetics and disorder properties of Be–Fe–Al intermetallics. Journal of Alloys and Compounds, 2015, 639, 111-122.	2.8	11
58	Thermal conductivity variation in uranium dioxide with gadolinia additions. Journal of Nuclear Materials, 2020, 540, 152258.	1.3	11
59	Hydrogen accommodation in the TiZrNbHfTa high entropy alloy. Acta Materialia, 2022, 229, 117832.	3.8	11
60	Density and structural effects in the radiation tolerance of TiO2polymorphs. Journal of Physics Condensed Matter, 2013, 25, 355402.	0.7	10
61	First-principles study of defects and fission product behavior in uranium diboride. Journal of Nuclear Materials, 2017, 494, 147-156.	1.3	10
62	Diffusion in doped and undoped amorphous zirconia. Journal of Nuclear Materials, 2021, 555, 153108.	1.3	10
63	Ion beam irradiation of ABO ₄ compounds with the fergusonite, monazite, scheelite, and zircon structures. Journal of the American Ceramic Society, 2020, 103, 5502-5514.	1.9	9
64	A high density composite fuel with integrated burnable absorber: U3Si2-UB2. Journal of Nuclear Materials, 2020, 529, 151891.	1.3	8
65	Swelling due to the partition of soluble fission products between the grey phase and uranium dioxide. Progress in Nuclear Energy, 2014, 72, 33-37.	1.3	7
66	Evidence of excess oxygen accommodation in yttria partially-stabilized zirconia. Scripta Materialia, 2020, 175, 7-10.	2.6	7
67	Transmutation of ABO4 compounds incorporating technetium-99 and caesium-137. Modelling and Simulation in Materials Science and Engineering, 2017, 25, 025011.	0.8	6
68	Experimental and computational assessment of U Si N ternary phases. Journal of Nuclear Materials, 2019, 516, 194-201.	1.3	6
69	Short communication on further elucidating the structure of amorphous U2O7 by extended X-ray absorption spectroscopy and DFT simulations. Journal of Nuclear Materials, 2020, 542, 152476.	1.3	5
70	Interface interactions in UN-X-UO2 systems (XÂ=ÂV, Nb, Ta, Cr, Mo, W) by pressure-assisted diffusion experiments at 1773 K. Journal of Nuclear Materials, 2022, 561, 153554.	1.3	5
71	Solubility and partitioning of impurities in Be alloys. Journal of Alloys and Compounds, 2016, 688, 382-385.	2.8	4
72	Coated ZrN sphere-UO2 composites as surrogates for UN-UO2 accident tolerant fuels. Journal of Nuclear Materials, 2022, 567, 153845.	1.3	4

#	Article	IF	CITATIONS
73	The accommodation of lithium in bulk ZrO2. Solid State Ionics, 2021, 373, 115813.	1.3	3
74	Self-contained dual-scale composite architectures in spray dried zirconium diboride. Ceramics International, 2022, 48, 17529-17538.	2.3	3
75	Ceramics in the nuclear fuel cycle. , 2020, , 63-87.		2
76	Ultrafast femtosecond laser micro-marking of single-crystal natural diamond by two-lens focusing system. Materials Today Communications, 2021, 26, 101800.	0.9	2
77	Predicting the thermal expansion of body-centred cubic (BCC) high entropy alloys in the Mo–Nb–Ta–Ti–W system. JPhys Energy, 2022, 4, 034002.	2.3	2
78	Accommodation and diffusion of Nd in uranium silicide - U3Si2. Journal of Nuclear Materials, 2021, 547, 152794.	1.3	0